Journal of Nano- and Electronic Physics
Vol. **18** No 4, 04021(5pp) (2026)

Журнал нано- та електронної фізики
Том **18** № 4, 04021(5cc) (2026)

OPEN ACCESS

REGULAR ARTICLE

Design and Analysis of Reconfigurable Dual Notched Ultra Wideband Microstrip Patch Antenna

Aritra Sinha[1], Tapas Tewary[2], Arindum Mukherjee[1], Sunandan Bhunia[1,*]

[1] *Department of ECE, Central Institute of Technology Kokrajhar, Assam, India*
[2] *Department of ECE, Academy of Technology, Hooghly, West Bengal, India*

(Received 15 March 2026; revised manuscript received 20 August 2026; published online 21 August 2026)

This study describes the design and implementation of a miniaturized ultra-wideband (UWB) microstrip patch antenna(MPA) intended for smart electronic systems, featuring two on-demand independently switchable band-notch attributes. The MPA is capable of suppressing a contiguous sub-band within WiMAX (3.2-3.8 GHz) and WLAN (5.1-5.8 GHz) band, as well as simultaneously mitigating both bands. Initially, a semicircular radiating plane combined with a altered partial ground plane is utilized to achieve the UWB characteristics while maintaining a small footprint. Two rejection bands are realized using two truncated circular slots on the patch. Equivalent circuits of PIN diode are employed to implement reconfigurability, providing ON-OFF control of each notch for adaptation to spectrum availability. The presented MPA exhibits a miniaturized physical footprint of 26 × 27 mm² and achieves a quasi-omnidirectional radiation characteristic with a peak gain of 4.6 dBi. The design also demonstrates a wide operational bandwidth (3-14 GHz) in the UWB spectrum, achieving a fractional bandwidth of 130 %. In terms of low profile, stable gain performance, and reconfigurable notch functionality, the proposed antenna shows satisfactory performance. Simulation results demonstrate stable radiation patterns, satisfactory gain performance, and strong suppression at the activated notched frequencies. Owing to its compact size, wide operational bandwidth, and flexible interference mitigation capability, the proposed design is suitable for UWB communication systems, cognitive radio applications, and portable wireless devices.

Keywords: Microstrip antenna, Reconfigurable notch, UWB, WiMAX, WLAN.

DOI: 10.21272/jnep.18(4).04021 PACS number: 84.40.Ba

1. INTRODUCTION

A reconfigurable notch-band antenna may dynamically modify its notch band properties to suppress certain narrowband (e.g., WiMAX, 5G, or WLAN) while maintaining ultra-wideband (UWB) or wideband performance. This flexibility is achieved by including switching devices like PIN diodes, MEMS switches, or varactor diodes. As a consequence, a single antenna may adapt to changing spectral environments, increasing flexibility and spectrum efficiency in smart communication systems [1-4]. A notch band antenna is generally an ultra-wideband (UWB) antenna engineered to operate across a very wide frequency spectrum while intentionally introducing one or more narrow stop-bands (notches). These notches remove interference from coexisting wireless services, such as Wi-Fi/WLAN, without compromising overall UWB performance. Precise band-rejection characteristics are commonly achieved using techniques like embedded slots, split-ring resonators (SRRs), or electromagnetic band-gap (EBG) structures [5-10]. Ref. [11] presents a frequency-reconfigurable monopole antenna for UWB and Ku-band applications. It uses Reuleaux-triangle microstrip-fed patch with a defective ground structure, where PIN diodes enable reconfigurability by altering the current distribution and effective electrical length. The antenna operates in two modes: a wide UWB band from 2.68-8.55 GHz (diodes OFF), covering WLAN (5.2 GHz), ISM (5.8 GHz), and lower X-band (~ 8 GHz), and a Ku-band from 12.7-15.65 GHz when the diodes are ON. Another frequency-reconfigurable antenna was proposed in [12] which operates at eight distinct frequencies depending on the switching states of three PIN diodes (S1, S2, S3). K. Dalal et al. in [13] proposed an UWB MPA by using a unique elliptical shaped radiating structure and a defected ground structure that encompasses a pair of L-shaped slots and two rectangular slots. The design features four notch bands: Wi-Max, WLAN, C-band and X-band. Five switches in ON/OFF states allows for reconfigurability of required notch-bands, making this design appropriate for a variety of narrowband applications. In [14] a compact ultra-wideband (UWB) antenna with reconfigurable triple band notch characteristics is proposed. The MPA has a CPW-fed circular shape patch and ground plane loaded with two slots in the form of 'C' shape and split-ring resonators (SRRs). Four PIN diodes are incorporated into the SRRs and slots. The antenna's current distribution in SRRs and slots allows for eight separate notch states, allowing UWB to coexist alongside 5G, X-band, WiMAX, WLAN without interfering. Developing tiny, low-profile antennas with integrated reconfigurable parts that preserve excellent performance and are ideal for seamless implantation in devices have been the main challenge or

* Correspondence e-mail: bhuniasunandan@gmail.com

Cite this article as: A. Sinha et al., *J. Nano- Electron. Phys.* 18 No 4, 04021 (2026) https://doi.org/10.21272/jnep.18(4).04021

research gap in this particular area.

This research work elaborates the design of a miniaturized reconfigurable UWB MPA with dual band-notched. Ultra-wideband operation is realized by modifying a conventional monopole antenna through the incorporation of a semi circular radiating plane and a truncated slot loaded ground plane. Two notch band characteristic for the WLAN band and WiMAX band is introduced using two truncated circular slots on the patch. Furthermore, notch reconfigurability is enabled through the integration of two PIN diodes. The design has been simulated in CST Studio Suite.

2. DESIGN, DEVELOPMENT OF PROPOSED ANTENNA

Fig. 1(a) and Fig. 1(b) depict the radiating plane and the ground structure of the projected antenna, respectively. 1.524 mm thick Rogers RO4730G3 (ε_r = 2.98, tan δ = 0.0029) is employed as the substrate layer. Radiating patch with semicircular in shape of radius R_1 mm is excited using a 50 Ohm microstrip feedline. The original ground plane, having the same dimensions as the substrate, is first reduced in length, and a rectangular slot (A × B) is then introduced at appropriate locations to form the final ground plane. Two truncated circular-shaped parasitic strips are etched out in the radiating patch, serving as a parasitic resonator that suppresses frequencies at WLAN (5.1-5.8 GHz) and WiMAX (3.2-3.8 GHz) band. Proposed antenna's variables and their values are tabulated in Table 1. Two PIN diodes are used as switches, shown in Fig. 1 are placed strategically on the slots to control the notch bands.

Table 1 Proposed MPA variable and their values (mm)

Variable	Value (mm)	Variable	Value (mm)	Variable	Value (mm)	Variable	Value (mm)
W_S	27	W_G	27	r_3	4.4	B	2
L_S	26	L_G	13.2	r_4	3.6	X	1
W_F	3.7	R_1	13	r_5	2.6	Y	0.5
L_F	13	r_2	5.4	A	4.4	–	–

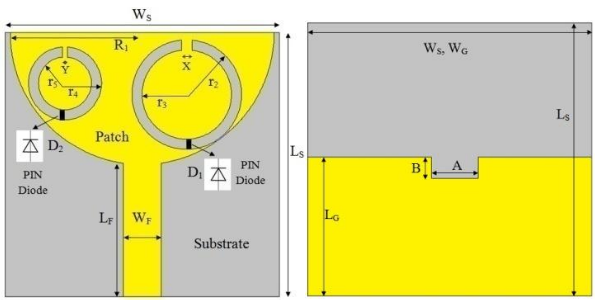

(a) (b)

Fig. 1 – Proposed MPA: (a) patch and (b) ground

3. DESIGN STEPS WITH SIMULATED RESULTS

Step-by-step evolution of proposed antenna design is illustrated in Fig. 2.

Step1: This configuration corresponds to the reference antenna described in the previous section. The reference circular patch radius '$R1$' was estimated for a resonant frequency of 5 GHz using traditional calculations.

$$R_1 = \frac{F}{\left(1+\frac{2h}{\pi\varepsilon_r F}\left(\ln\left(\frac{\pi F}{2h}\right)+1.7726\right)\right)^{\frac{1}{2}}},$$

where

$$F = \frac{8.791\times10^9}{f_r\sqrt{\epsilon_r}},$$

where h – substrate height, ϵ_r – dielectric constant

The Fractional Bandwidth Ratio (%FBR) is calculated using:

$$FBR(\%) = \frac{F_U-F_L}{F_C} \times 100\ \%.$$

Where, F_L = 3 GHz is the lower cutoff frequency, upper cutoff frequency F_U = 14 GHz, and $F_C = (F_U + F_L)/2$ is the = Center frequency. Accordingly, the reference antenna achieves a fractional bandwidth of approximately 130 %.

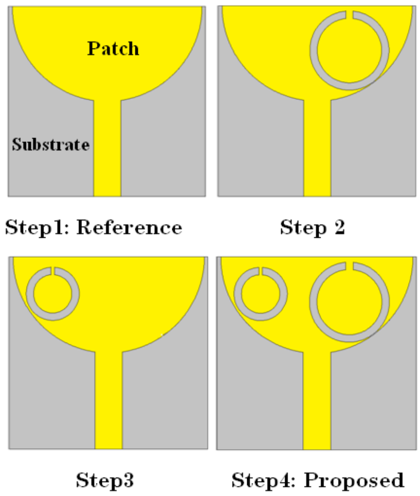

Fig. 2 – Proposed MPA's Evolution steps

Step2 and Step 3: This step results in a UWB antenna incorporating two band-notch characteristics. Two truncated ring slots etched on the semicircular radiating patch, as shown in Step 2-3 of Fig. 2, are responsible for generating the frequency rejection bands. One annular slot with a radius of 4.9 mm, slot width of 1 mm, and a top-end opening of 0.5 mm is designed to reject the WiMAX (3.2-3.8 GHz) frequency band. The second circular slot, having a radius of 3.1 mm and a slot width of 1 mm with a top-end opening of 0.2 mm, is employed to generate the notch in WLAN (5.1-5.8 GHz) band.

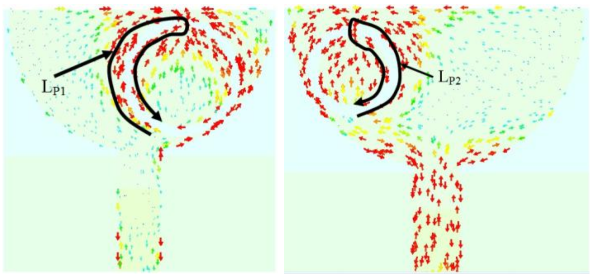

(a) (b)

Fig. 3 – Effective surface current path along circular slots:

(a) 3.5 GHz (b) 5.5 GHz

Fig. 3 exhibits the approximate current path length around the slots in one direction. The required value of effective current path length L_{P1} and L_{P2} for a central frequency can be calculated using the following equation:

$$f_{notch} = \frac{C}{2L_P\sqrt{\frac{\varepsilon_r+1}{2}}}$$

Where, C and f_{notch} are velocity of light in free space and notch band center frequency of the respectively, and ε_r is the permittivity of the substrate. Accordingly, the effective current path length L_{P1} is calculated as 26 mm approximately for 3.5 GHz and 16 mm for the 5.5 GHz.

Step4: In this step, both circular slots are employed to achieve the dual notched Ultrawideband characteristics.

A parametric sweep available in the simulation software is employed to identify the optimum slot-opening lengths for the targeted notch frequency ranges.

4. RECONFIGURABILITY WITH PIN DIODE

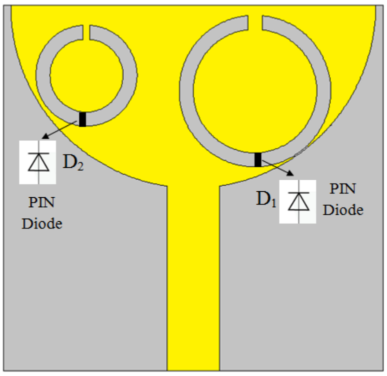

Fig. 4 – PIN diodes to control notch bands

In this final step, the dual band-notched antenna obtained in Step 4 is modified to achieve independent reconfigurability of the notch bands by employing two PIN diodes. Each PIN diode is connected across the two top edges of the corresponding slot, at half length of the slot. PIN diode's RLC equivalent circuit in ON state and OFF state are shown Fig. 5. The RLC parameters of a PIN diode vary with bias: in the ON (forward bias) state, it behaves as a low resistance (approximately 1-2 Ω) in series with a minor parasitic inductance (in the nH range), whereas in the OFF (reverse bias) state, it functions as a high resistance (in kΩ or more range) in series with junction capacitance (in the pF range) and the same parasitic inductance, rendering it as a variable resistor advantageous for RF switching and attenuation. When a PIN diode is in the ON state, it effectively short-circuits the corresponding slot, neutralizing the effective current path length and thereby disabling the associated notch band. Conversely, when the diode is in the OFF state, the slot remains electrically effective and continues to produce the desired band-notch response. Table 2 shows typical values of R, L, C used for simulation for simulation environment. Table 3 tabulates the simulation outcomes for four different conditions of diodes.

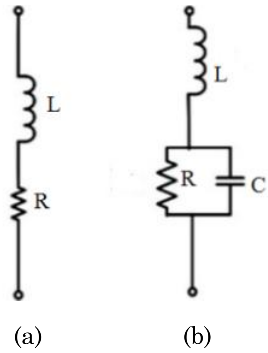

Fig. 5 – RLC circuit of PIN diode (a) ON and (b) OFF state

ON-OFF control of the two PIN diodes is independent of each other, enabling multiple reconfigurable operating states. As a result, the antenna can operate in four distinct reconfigurable states, as illustrated in Fig. 6.

Table 2 – R, L, C values for PIN diodes in 'ON' and 'OFF' condition

Diode State	R (Resistor)	L (Inductor)	C (Capacitor)
ON	2 Ω	0.6 nH	negligible
OFF	1 MΩ	0.6 nH	0.02 pF

Table 3 – Outcomes in four different conditions of diodes

Diode Condition		Outcome
1	D_1 = ON, D_2 = ON	Continuous UWB operation with no notched bands
2	D_1 = ON, D_2 = OFF	Notch band corresponding to the WiMAX (3.2-3.8 GHz) is activated
3	D_1 = OFF, D_2 = ON	Notch band corresponding to the WLAN(5.1-5.8GHz) is activated
4	D_1 = OFF, D_2 = OFF	Simultaneous rejection of both WiMAX and WLAN bands are activated

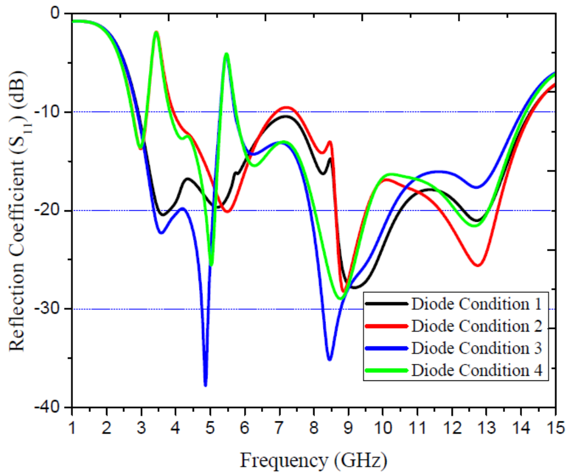

Fig. 6 – Variation of S_{11} for diode switch conditions

A comparison of the peak gain and efficiency for all four reconfigurable states is shown in Fig. 7 and Fig. 8 respectively. As expected, activation of the notch bands leads to a reduction in gain and efficiency.

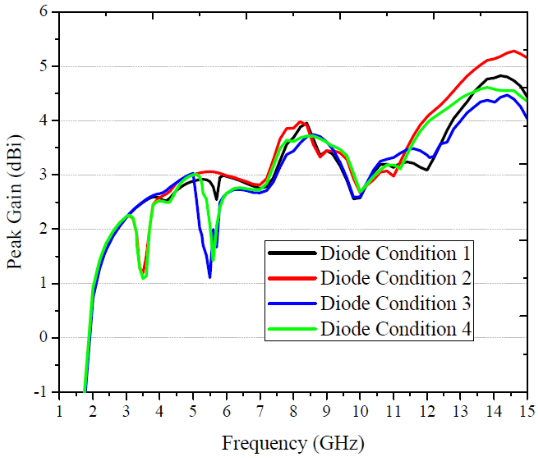

Fig. 7 – Variation of peak gain for diode switch conditions

Fig. 9 and 10 show radiation pattern (absolute) both in *E* and *H* plane, at two notch band frequencies (3.5 and 5.5 GHz) and one pass-band resonant frequency (8.6 GHz). The radiation pattern shows that gains at two notch frequencies are much lower than those at the pass-band resonant frequency.

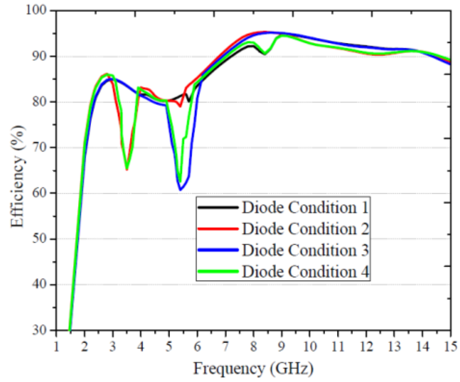

Fig. 8 – Variation of efficiency (%) for diode switch conditions

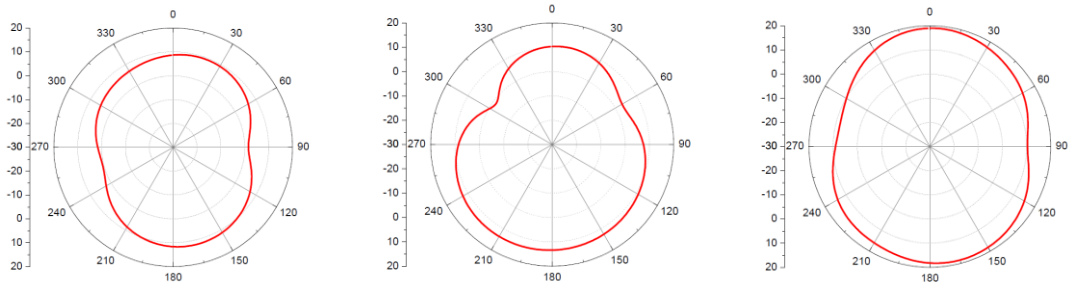

(a) (b) (c)

Fig. 9 – *E* plane radiation patterns at (a) 3.5 (b) 5.5 and (c) 8.6 GHz

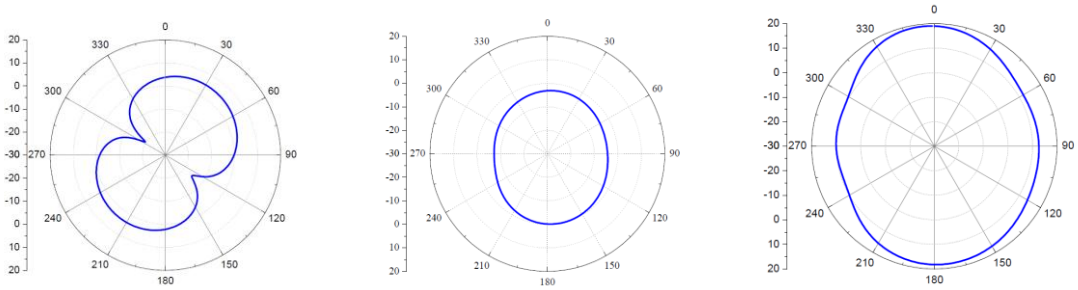

(a) (b) (c)

Fig. 10 – *H* plane radiation patterns at (a) 3.5 (b) 5.5 and (c) 8.6 GHz

5. CONCLUSION

A miniaturized planar UWB microstrip antenna with two independently reconfigurable band-notch characteristics has been presented in this work. The planned antenna employs a semicircular radiating patch and modified partial ground plane to achieve wide bandwidth, while two truncated circular slots in the radiating patch are introduced for realizing dual band rejection. Independent control of the notched bands is accomplished using PIN diodes, enabling dynamic adaptation to spectral requirements. The presented MPA operates over frequency range of 3-14 GHz, achieving a fractional bandwidth of approximately 130 %. Around 18 dB isolation has been achieved between notches and pass band of the antenna. Four distinct reconfigurable states are realized by selectively switching the PIN diodes, allowing the antenna to suppress either or both Wi-MAX and WLAN bands without affecting the overall UWB performance.

REFERENCES

1. E. García, A. Andújar, J. Anguera, *Electronics* **13** No 20, 3988 (2024) https://doi.org/10.3390/electronics13203988.
2. H.C. Mohanta, A. Kouzani, S. Mandal, *Univ. J. Elect. Electron. Eng.* **6**, 239 (2019) https://doi.org/10.13189/ujeee.2019.060406.
3. S. Dubal, A. Chaudhari, *2020 10th International Conference on Cloud Computing, Data Science & Engineering (Confluence)*, 576 (Noida, India: 2020).
4. A.A. Vaganova, N.N. Kisel, A.I. Panychev, *2021 Radiation and Scattering of Electromagnetic Waves (RSEMW)*, 127 (Divnomorskoe, Russia: 2021).
5. S. Mukherjee, A. Roy, S. Bhunia, *J. Nano- Electron. Phys.* **13** No 3, 03026 (2021) https://doi.org/10.21272/jnep.13(3).03026.
6. S. Mukherjee, A. Roy, S. Maity, T. Tewary, P.P. Sarkar, S. Bhunia, *Int. J. Microwave Wireless Technol.* **15**, 526 (2023) https://doi.org/10.1017/S1759078722000447.
7. S. Mukherjee, A. Roy, S. Maity, T. Tewary, K. Dutta, S. Bhunia, *Int. J. Commun. Syst.* **36** No 15, e5565 (2023) https://doi.org/10.1002/dac.5565.
8. T. Tewary, A. Mukherjee, S. Bhunia, *J. Nano- Electron. Phys.* **16** No 5, 05013 (2024) https://doi.org/10.21272/jnep.16(5).05013.
9. S. Mukherjee, A. Roy, A. Mukherjee, S. Kundu, P.P. Sarkar, S. Bhunia, *AEU – Int. J. Electron. Commun.* **178**, 155276 (2024) https://doi.org/10.1016/j.aeue.2024.155276.
10. S. Mukherjee, A. Roy, T. Tewary, K. Mandal, P.P. Sarkar, S. Bhunia, *Int. J. Commun. Syst.* **37** No 12, e5814 (2024) https://doi.org/10.1002/dac.5814.
11. S.E. Bayer Keskin, S. Koziel, S. Szczepanski, *Sci. Rep.* **15**, 6555 (2025) https://doi.org/10.1038/s41598-025-91108-7.
12. K. Karthika, K. Kavitha, A. Aparna, A.D. Mary, N. Rithanya, *2022 8th International Conference on Advanced Computing and Communication Systems (ICACCS)*, 793 (Coimbatore, India: 2022).
13. K. Dalal, T. Singh, P.K. Singh, *Wireless Pers. Commun.* **125** No 2, 1405 (2022) https://doi.org/10.1007/s11277-022-09611-3.
14. L. Li, J. Nan, J. Liu, C. Tao, *Int. J. Microwave Wireless Technol.* **13** No 8, 826 (2021) https://doi.org/10.1017/S1759078720001580.

Проєктування та аналіз реконфігурованої подвійної надширокосмугової мікросмужкової антени з надширокосмуговим вирізом

Aritra Sinha[1], Tapas Tewary[2], Arindum Mukherjee[1], Sunandan Bhunia[1]

[1] *Department of ECE, Central Institute of Technology Kokrajhar, Assam, India*
[2] *Department of ECE, Academy of Technology, Hooghly, West Bengal, India*

У роботі описано проєктування та реалізація мініатюрної надширокосмугової (UWB) мікросмужкової патч-антени (МПА), призначеної для інтелектуальних електронних систем, що має два незалежно перемикані на вимогу атрибути смуги-вирізу. МПА здатна придушувати суміжний піддіапазон у діапазоні WiMAX (3,2-3,8 ГГц) та WLAN (5,1-5,8 ГГц), а також одночасно пом'якшувати обидві смуги. Спочатку для досягнення характеристик UWB, зберігаючи при цьому малу площину, використовується напівкругла випромінювальна площина в поєднанні зі зміненою частковою площиною заземлення. Дві смуги регенування реалізуються за допомогою двох усічених круглих пазів на патчі. Для реалізації реконфігурації використовуються еквівалентні схеми PIN-діода, що забезпечує керування вмиканням/вимиканням кожної вирізки для адаптації до доступності спектру. Представлена МПА демонструє мініатюрну фізичну площу 26 × 27 мм² та досягає квазівсенаправленої характеристики випромінювання з піковим коефіцієнтом посилення 4,6 дБі. Конструкція також демонструє широку робочу смугу пропускання (3-14 ГГц) у спектрі надширокого діапазону (UWB), досягаючи часткової смуги пропускання 130 %. З точки зору низького профілю, стабільних характеристик посилення та реконфігурованої функціональності режекції, запропонована антена демонструє задовільні характеристики. Результати моделювання демонструють стабільні діаграми спрямованості, задовільні характеристики посилення та сильне придушення на активованих режекторних частотах. Завдяки компактним розмірам, широкій робочій смузі пропускання та гнучким можливостям зменшення перешкод, запропонована конструкція підходить для систем зв'язку UWB, застосувань когнітивного радіо та портативних бездротових пристроїв.

Ключові слова: Мікросмужкова антена, Реконфігурована виїмка, Надширокий діапазон (UWB), WiMAX, WLAN.